

Modeling of nonlinear response of R/C shear deficient t-beam subjected to cyclic loading

R.A. Hawileh¹, J.A. Abdalla*¹ and M.H. Tanarslan²

¹Department of Civil Engineering, American University of Sharjah, Sharjah, UAE

²Department of Civil Engineering, Dokuz Eylul University, Buca, Izmir 35160, Turkey

(Received September 30, 2011, Revised March 19, 2012, Accepted May 8, 2012)

Abstract. This paper presents a finite element (FE) model for predicting the nonlinear response and behavior of a reinforced concrete T-beam deficient in shear under cyclic loading. Cracking loads, failure loads, response hysteresis envelopes and crack patterns were used as bench mark for comparison between experimental and FE results. A parametric study was carried out to predict the optimum combination of the open and close crack shear transfer coefficients (β_o and β_c) of the constitutive material model for concrete. It is concluded that when both shear transfer coefficients are equal to 0.2 the FE results gave the best correlation with the experimental results. The results were also verified on a rectangular shear deficient beam (R-beam) tested under cyclic loading and it is concluded that the variation of section geometry has no effect on the optimum choice of the values of shear transfer coefficients of 0.2. In addition, a parametric study based on the variation of concrete compressive strength, was carried out on the T-beam and it is observed that the variation of concrete compressive strength has little effect on the deflection. Further conclusions and observations were also drawn.

Keywords: reinforced concrete; finite element modeling; shear deficient T-beam; cyclic load.

1. Introduction

Shear failure in reinforced concrete beams is one of the most undesirable failure modes due to its severity and brittleness. In addition, in spite of numerous experimental programs that were carried out to investigate shear in beams, it still remains as one of the areas of continuous research. This is mainly due to complexity of shear behavior. To have good understanding of shear behavior of beams, experimental based testing is needed and it is very valuable and indispensable. Test results usually give insight information about the behavior, real life response and strength of the tested specimen, however, they are time consuming and costly. Therefore, it is desirable to develop reliable analytical or numerical approaches that can serve as a supplement and in some case as an alternative to experimental testing. There are numerous methods for modeling concrete structures using both analytical and numerical approaches. The well known finite element analysis is the most widely used numerical method for analyzing concrete structures when the material behaves nonlinearly.

To achieve reliable finite element results that compares well with the experimental results, the finite element model must closely represents the dimension, boundary conditions and material properties – especially the material nonlinearity. In general, the nonlinear response of the reinforced

* Corresponding author, Professor, E-mail: jabdalla@aus.edu

concrete structure is caused by two major factors, cracking of the concrete and plastic behavior of reinforcement. In order to simulate the relationship between the reinforced concrete and reinforcing steel, perfect bond between the concrete and steel was assumed. Defining bond as perfect is the most common method used for finite element definition.

Modeling concrete behavior and using it in the finite element analysis received considerable attention over the last two decades. Several material models have been proposed and used by many researchers to numerically investigate the behavior of beams and compare them with the experimental results (Kotsovos and Pavlovic 1986, Kwak and Filippou 1990). Nilson (1968) used nonlinear material properties of concrete and steel to model a RC structure and included the effects of cracking based on a pre-defined crack pattern. Kwak and Filippou (1990, 1997) modeled the monotonic behavior of reinforced concrete beams, slabs and beam-column joint sub-assemblages using finite element analysis. A smeared crack finite element model was proposed based on an improved cracking criterion and nonlinear solution scheme, which is derived from fracture mechanics principles. The finite element results were compared with experimental results and showed good agreement. Hu and Schnobrich (1990) derived a set of constitutive equations suitable for cracked RC structures subjected to in-plane shear and normal stresses. The proposed model took into account the smeared crack representation, rotating-crack approach, tension stiffening, stress-degrading effect for concrete parallel to the crack direction and shear retention of concrete on the crack surface. The proposed material model has been tested and validated against experimental data and demonstrated its adequacy in describing the post-cracking behavior of reinforced concrete element.

Al-Ta'an and Ezzadeen (1995) developed a numerical procedure based on finite element method which considers the geometric and material nonlinear analysis of reinforced concrete members. The numerical solutions of a number of reinforced fibrous concrete beams were compared with published experimental test results and showed a good agreement. Bhatt and Kader (1998) presented a 2D finite element parabolic isoparametric quadrilateral element for predicting the shear strength of RC rectangular beams based on the tangent stiffening method. Fanning (2001) analyzed reinforced and post tensioned concrete beams using the smeared crack models implemented in ANSYS (2007). The models were validated with experimental load-deflection responses and showed good correlation. The study concluded that the dedicated ANSYS smeared crack model is an appropriate numerical model for capturing the flexural modes of failure of reinforced concrete systems and accurately predicts the deflection and ultimate strength of reinforced concrete systems. Many researchers have used the existing finite element programs including ANSYS and others program for nonlinear analysis of reinforced and prestressed concrete members and structures (Cela 1998, Hawileh *et al.* 2010, Cotsovos *et al.* 2009, Masti 2009, Hawileh *et al.* 2009, Hawileh *et al.* 2010, Hawileh *et al.* 2011, Huang *et al.* 2010, Kim *et al.* 2010, Naser *et al.* 2011).

Although shear behavior of beams under monotonic loading had received considerable attention, limited research has been conducted on the behavior of shear deficient beams under cyclic loading. Tanarslan and Altin (2010) conducted an extensive experimental program to investigate, among other things, the effects of CFRP on behavior and on ultimate strength of shear deficient (without stirrups) reinforced concrete (RC) beams. One of the tested specimens is a T-beam without shear reinforcement or external CFRP. This beam is used as the control beam to compare the behavior of other beams reinforced with external CFRP. In this study a finite element model was developed for the T-beam and the experimental results of Tanarslan and Altin (2010) were used to validate the finite element model. The finite element analysis package ANSYS (2007) has been used and its

results were compared with the test results. First cracking loads, loads at failure, response envelopes based on load-deflection and crack patterns were taken into account for comparison. This study indicated that the use of finite element program to model experimental data is viable and the results that are obtained from analysis can indeed model RC beam behavior that is deficient in shear under earthquake cyclic loading reasonably well. A parametric study was then carried out to investigate the effect of the open and closed shear transfer coefficients on the response of the finite element model. These coefficients are needed for the constitutive concrete nonlinear material model of the tested beam. Further parametric study was carried out on the T-beam to investigate the effect of variation of the concrete compressive strength on deflection. Although many investigators have used the finite element to model shear response of reinforced concrete beams under monotonic loading as indicated above, investigation of shear response of reinforced concrete members under cyclic loading received less attention. This paper specifically model and analyze the behavior of shear deficient T-beam under cyclic load and validate it with experimental results.

2. Experimental program

A cantilever reinforced concrete T-beam with a total span of 1750 mm was designed based on ACI 318-05 code (2005) and tested by Tanarlsan and Altin (2010) in an experimental program. As shown in Fig. 1, the T-beam has a flange width of 360 mm and a flange thickness of 75 mm, a web thickness of 120 mm and a total depth of 360 mm. It is reinforced with three 20 mm diameter deformed steel bars in the compression zone and three 20 mm diameter deformed steel bars in the tension zone. The T-beam was designed to have deficiency in shear capacity, i.e., it has no internal or external shear reinforcements. However, stirrups were provided outside the shear span to prevent the formation of local cracks in the vicinity of the applied load and may consequently leads to premature failure. The provided shear reinforcement in the vicinity of the load consisted of four 6

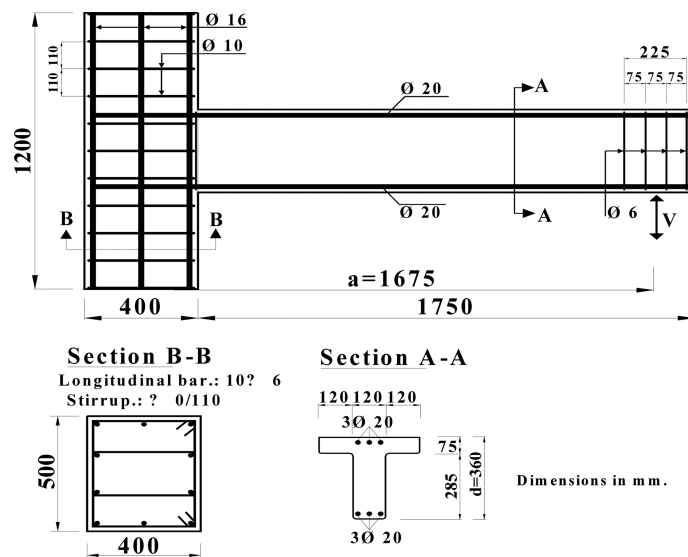


Fig. 1 Geometry and reinforcement details of the tested T-beam (Tanarlsan *et al.* 2010)

mm diameter stirrups at 75 mm center to center. The rest of the dimensions and reinforcement details are shown in Fig. 1. The tested cantilever T-beam was supported by a strong wall with rigid support at its end with the help of two 45 mm diameter high strength steel mounting rods.

To apply cyclic load to the cantilever T-beam, a loading column was designed with hinges by the beam's free end. The loading column contained two hinges, a load cell and a hydraulic jack. The capacity of the hydraulic jack was 1000 kN while the load cell's capacity was 600 kN. The load was applied in cycles of loading and unloading. After applying a couple of cycles in elastic region, flexural and shear cracks developed. Loading was continued until the T-beam reached its ultimate load capacity. At each increment of load, deflection changes were measured using the LVDT located at the free end of the cantilever T-beam to measure maximum deflection. Details of the instrumentation and experimental settings were given in Tanarslan and Altin (2010).

3. Mathematical modeling (Approximate equations)

The purpose of this section is to show how the shear transfer coefficients β_t for open crack (tension) and β_c for close crack (compression) influence the concrete material constitutive relation. The concrete material constitutive law is given by Zeinkiewicz *et al.* (2005).

$$\{\sigma\} = [D_c](\{\varepsilon\} - \{\varepsilon_0\}) + \{\sigma_0\} \quad (1)$$

where, $[D_c]$ is the concrete material stress-strain matrix, $\{\varepsilon_0\}$ is the initial strain vector and $\{\sigma_0\}$ is the initial stress vector. The concrete material stress-strain matrix ($[D_c]$) is a function of modulus of elasticity (E) and Poisson's ratio (ν) of concrete. When concrete cracks, the material stress-strain matrix get modified by introducing shear strength reduction factors represented by two shear transfer coefficients β_t for open crack and β_c for close crack. In addition, in the case of open crack a second parameter R' that specifies secant modulus (slope) is introduced and it diminishes to 0 as the solution converges. The two modified stress-strain matrices for open and close cracks are given by Eqs. (2) and (3), respectively. More details of the formulation are given in ANSYS (2007).

$$[D_c^{ck}] = \frac{E}{(1+\nu)} \begin{bmatrix} \frac{R'(1+\nu)}{E} & 0 & 0 & 0 & 0 & 0 \\ 0 & \frac{1}{(1-\nu)} & \frac{\nu}{(1-\nu)} & 0 & 0 & 0 \\ 0 & \frac{\nu}{(1-\nu)} & \frac{1}{(1-\nu)} & 0 & 0 & 0 \\ 0 & 0 & 0 & \frac{\beta_t}{2} & 0 & 0 \\ 0 & 0 & 0 & 0 & \frac{1}{2} & 0 \\ 0 & 0 & 0 & 0 & 0 & \frac{\beta_t}{2} \end{bmatrix} \quad (2)$$

$$[D_c^{ck}] = \frac{E}{(1+\nu)(1-2\nu)} \begin{bmatrix} (1-\nu) & \nu & \nu & 0 & 0 & 0 \\ \nu & (1-\nu) & \nu & 0 & 0 & 0 \\ \nu & \nu & (1-\nu) & 0 & 0 & 0 \\ 0 & 0 & 0 & \beta_c \frac{(1-2\nu)}{2} & 0 & 0 \\ 0 & 0 & 0 & 0 & \frac{(1-2\nu)}{2} & 0 \\ 0 & 0 & 0 & 0 & 0 & \beta_c \frac{(1-2\nu)}{2} \end{bmatrix} \quad (3)$$

By applying the theorem of minimum potential energy or the virtual work principle, and ignoring the effect of initial strain, initial stress, surface force and body force, after further simplifications, the stiffness matrix can be written as follows

$$[K] = \sum_{ele} [B]^T [D_c^{ck}] [B] dV \quad (4)$$

where, $[B]$ is the strain-displacement matrix. Since reinforced concrete consists of both concrete and steel, the stiffness matrix of reinforced concrete must include both the concrete and reinforcing steel properties. This can be achieved by superposition of concrete and reinforcing steel stiffness matrices. The standard nonlinear analysis procedure was followed in which load will be applied incrementally, linear approximation and correction with each load increment will be carried out and iteratively the final solution will be reached at a specified convergence ANSYS (2007). Failure is assumed to occur at the onset of the steel reinforcement yielding.

4. Finite element model

4.1 Elements and geometry modeling

The studied finite element model of the cantilever T-beam has similar dimensions, material properties, geometry configuration, boundary conditions and loading as that of the test specimen shown in Fig.

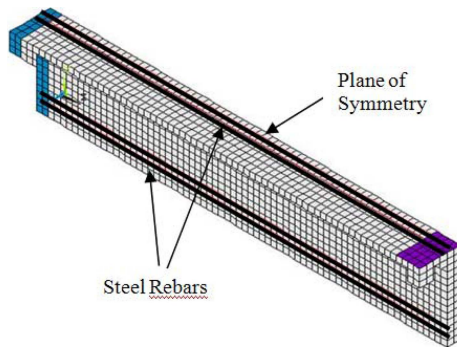


Fig. 2 3D Finite element isometric view of the T-beam

1. The finite element analysis in this study is performed using ANSYS 11.0 (2007). Making use of symmetry in geometry, materials and loading, only half of the full T-beam was used for modeling and loadings resulting in a significant reduction of computational time. The model was developed in ANSYS WORKBENCH Version 11.0 (2007). Both the geometry and mesh of the modeled cantilever T-beam are shown in Fig. 2.

To model nonlinear behavior of concrete an eight-node solid element, SOLID65 ANSYS (2007) was used. This element has the capability to model cracking in three orthogonal direction, crushing and plastic deformation. Each node has three degrees of freedom. The solid element has also translational degrees of freedom in the nodal x , y and z directions. The link element LINK8 ANSYS (2007) was used to model the discrete steel reinforcement bars as shown in Fig. 2. The element is capable of elastic-plastic deformation, stress stiffening and large deflection. Each link element has two nodes and each node has three translational degrees of freedom in the nodal x , y and z directions. Ideally, the slip between the steel reinforcement and concrete would be taken into account but according to Park and Kim (2005) and Obidat *et al.* (2010) perfect bond between the reinforcement steel and concrete is a valid assumption and was used herein. In order to provide perfect bond assumption between the concrete and steel, nodes of the LINK8 steel elements were connected to those of adjacent concrete SOLID65 elements by sharing the same nodes. In addition, the ASCE state of art report (1982) showed that dowel action of flexural reinforcement is generally not dominant in beams with proportional dimensions where such an effect has to be taken into account in cases of deep beams and the presence of large sizes of flexural reinforcement. Thus, the author assumed that dowel action in this study has a minimal effect and was not considered in this study. The solid element SOLID45 is used to model the steel plate under the applied load and at the support in the T-beam model. SOLID45 is an eight-node solid element having three degrees of freedom per node similar to that of SOLID65 element ANSYS (2007). A total of 2800 SOLID65 concrete elements and 264 LINK8 elements for top and bottom reinforcement are used to model the tested cantilever T-beam.

4.2 Material modeling and properties

In the finite element analysis, cracking occurs in a concrete element when the principal tensile stress in any direction lies outside the failure surface. After cracking, the concrete material is assumed to behave as an orthotropic material and the elastic modulus of the concrete element is set to zero in the direction parallel to the principal tensile stress direction. The post cracking tensile behavior of the concrete material is adopted in the FE model by using a bilinear softening stress-strain response. Crushing occurs when all principal stresses are compressive and lie outside the failure surface (Cotsovos *et al.* 2009) consequently, the elastic modulus is set to zero in all directions and the element local stiffness becomes zero resulting in large displacement and therefore divergence in the solution.

Defining the nonlinear material properties of reinforced concrete structure is very crucial to accurately simulate the behavior of the T-beam. Basically, the nonlinear response of the RC structure is caused by two major factors, cracking of the concrete and plasticity of the reinforcement steel re-bars. Up to the first crack of concrete, the behavior is linear but afterwards it becomes nonlinear. The uncracked elastic stage and cracked plastic stage of the concrete had to be treated separately. Also the behavior of the reinforced steel had to be defined perfectly.

To predict the response of the experimental work, a finite element model reflecting the beam

material's properties had to be developed. Compressive strength of concrete and tensile strength of steel reinforcement, used as ANSYS input data, were based on the T-beam's material properties obtain from test results. Compressive and tensile strength and modulus of elasticity of concrete were taken as the measured experimental values of 30.3 MPa, 3.43 MPa and 26050 MPa, respectively and a Poisson's ratio of 0.2 is used. To define the plastic behavior of concrete, a multi-linear compressive stress-strain curve was defined according to a model that discussed in a subsequent section. The multi-linear isotropic material uses the Von Mises failure criterion along with the William and Warnke (1975) model to define the failure of the concrete.

Additional concrete material data, such as the shear transfer coefficients (β_i and β_c) are also needed for the concrete material data table. Typical shear transfer coefficients are taken as zero when there is a total loss of shear transfer, i.e., representing smooth crack and 1.0 when there is no loss of shear transfer, i.e., representing rough crack ANSYS (2007). This specification was made for both the open and the close crack presented by β_i for an open crack and β_c for a closed crack, respectively. An extensive parametric study that will be discussed in a subsequent section has been conducted in this study to find the optimum combinations of these two coefficients to predict the experimental results. The other parameter needed for William and Warnke (1975) model is the stiffness multiplier for cracked tensile condition. The bilinear softening stress-strain response mentioned earlier has linearly ascending segment up to the concrete rupture stress. Once the concrete material reaches its tensile peak stress, a tensile stiffness multiplier of 0.6 is used to simulate a sudden drop of the tensile stress to 60% of the rupture stress; followed by a linearly descending curve to zero stress at a strain value of six times the strain corresponding to the concrete rupture stress.

The steel was assumed to be an elastic-perfectly plastic material. Von Misses failure criteria were used to simulate the yielding of the reinforcing steel bars. The steel's modulus of elasticity and yield stress were taken as 205 GPa and 414 MPa, respectively and a Poisson's ratio of 0.3 is used.

4.3 Concrete nonlinear material model

Concrete is a quasi-brittle material and has different behavior in compression and tension, therefore developing a nonlinear material model for concrete that captures all its behavior accurately is not an easy task. The compression part of the stress-strain curve for concrete extends linearly for up to about 30% of the maximum compressive strength. Above this point, the stress increases gradually and nonlinearly up to the maximum compressive strength. The tension part of the stress-strain curve is linear elastic up to the maximum tensile strength. After this point, the concrete cracks and the strength decreases gradually to zero. The tensile strength of concrete is usually about 10% on average of the compressive strength of concrete. The concrete tensile strength is taken equal to the concrete rupture strength f_r . The tensile strengths for the tested T-beam model were calculated using Eq. (5) (Desayi and Krishnan 1964, Bangash 1989, Kachlakev 2002, Chen 2006).

$$f_r = 0.623\sqrt{f_c'} \tag{5}$$

where,

f_c' = ultimate concrete compressive strength, MPa

f_r = ultimate concrete tensile strength (modulus of rupture), MPa

The uniaxial stress-strain relationship for concrete in compression is simulated with multilinear isotropic hardening material. Eqs. (6) and (7) are used to construct the uniaxial compressive stress-

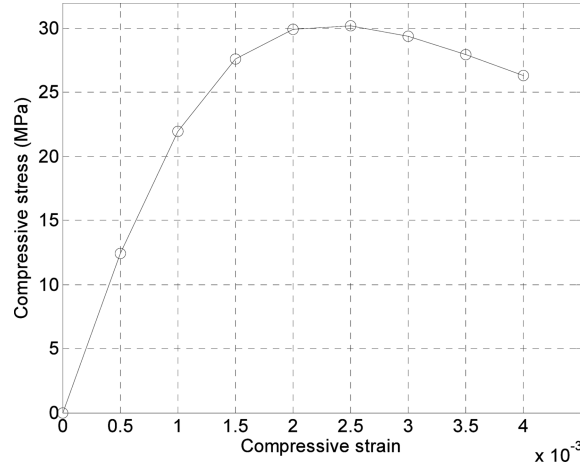


Fig. 3 Idealized uniaxial compressive stress-strain curve for concrete

strain curve for the concrete material (Desayi and Krishnan 1964, Bangash 1989).

$$f = \frac{E_c \varepsilon}{1 + \left(\frac{\varepsilon}{\varepsilon_0}\right)^2} \quad (6)$$

$$\varepsilon_0 = \frac{2f'_c}{E_c} \quad (7)$$

where,

$$E_c = 4730 \sqrt{f'_c}, \text{ MPa}$$

f = stress at any strain ε (MPa)

ε = strain at stress f

ε_0 = strain at the ultimate compressive strength f'_c

Fig. 3 shows the developed compressive uniaxial stress-strain relationship for concrete based on this material model. This concrete stress-strain curve is used in modeling the finite elements.

4.4 Boundary conditions and loads

In the experimental setup, the boundary conditions were as follows: one end of the T-beam is fixed and the other end is free. The boundary conditions were assigned in the finite element model to accurately represent the experimental setup shown in Fig. 4. Nodes at the T-beam's fixed end are restrained in the horizontal x -direction, vertical y -direction and lateral z -direction. Symmetry is modeled by restraining the T-beam with rollers along the axis of symmetry. One plane of symmetry was defined and the displacement perpendicular to the plane of symmetry was constrained to zero. A cyclic loading history is applied at the free end of the cantilever T-beam. The applied cyclic loading is shown in Fig. 5. This is presented in the finite element model by applying the load as a function of time at the free end of the beam as shown in Fig. 4.

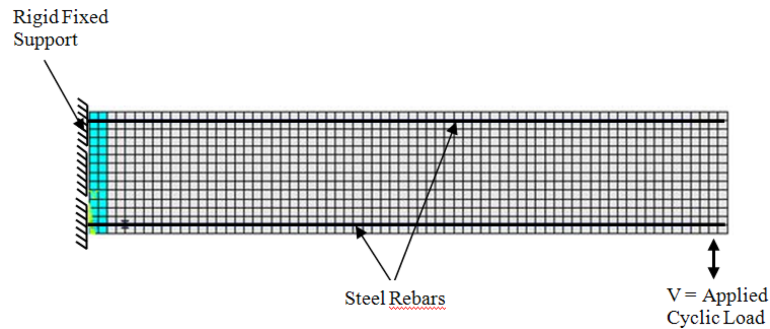


Fig. 4 Finite element model with boundary conditions and loading

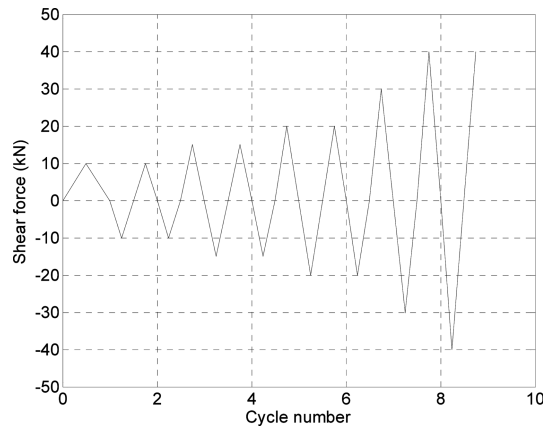


Fig. 5 Applied load cycles for the T-beam

4.5 Non-linear solution and convergence criteria

The applied cyclic loads were divided into a series of load increments called load steps and substeps. At the end of each load increment, convergence is achieved by Newton-Raphson equilibrium iterations within tolerance limits of the convergence criteria are satisfied. In this study, automatic time stepping option is turned on to predict and to control load step sizes. The convergence criteria were based on force and displacement, and ANSYS convergence default values of 0.5% were initially selected. Convergence was difficult to achieve using the ANSYS default values due to the nonlinear behavior of the concrete element and large deflections. Thus, the convergence tolerance limits were increased by one order of magnitude (0.05 for force and displacement checking) in order to obtain convergence of the solutions.

5. Results and discussions

5.1 Comparison of numerical and experimental results

The test was carried out under cyclic loading. Instead of comparing every load cycle, response envelopes were constructed for comparison. Response envelopes were drawn by connecting peak

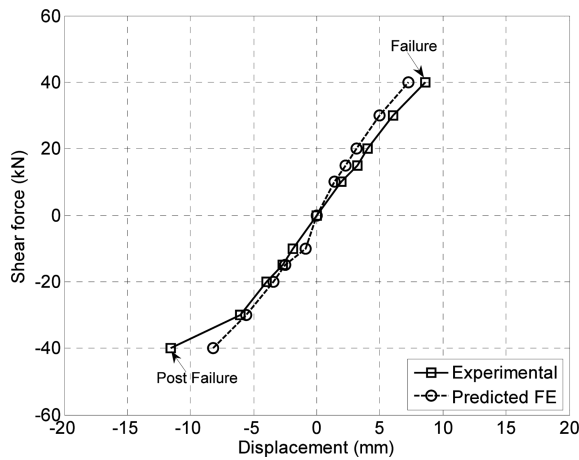


Fig. 6 Applied load versus measured and predicted displacement of the T-beam ($\beta_t = 0.2$, $\beta_c = 0.2$)

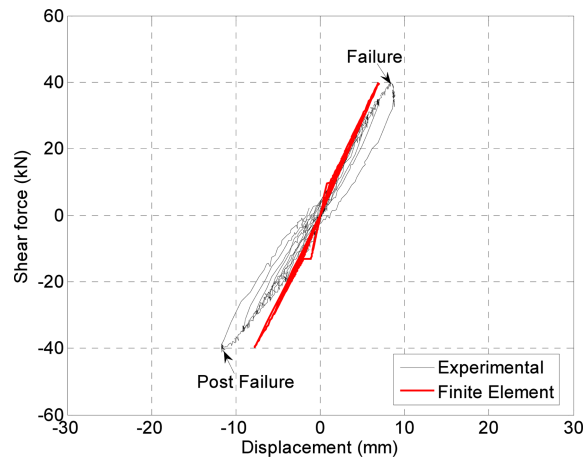


Fig. 7 Response hysteresis envelopes of the T-beam ($\beta_t = 0.2$, $\beta_c = 0.2$)

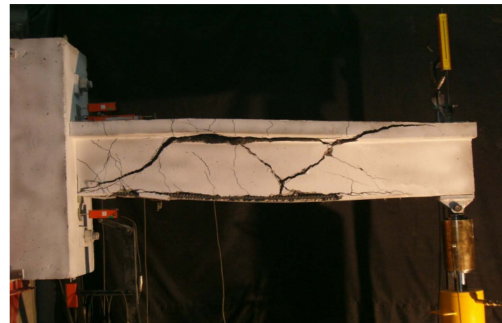
points of the loading cycles. The response envelope for the free end span deflection of the tested T-beam and the predicted response from the finite element model are presented and compared in Fig. 6 for $\beta_t = 0.2$ and $\beta_c = 0.2$. In addition, Fig. 7 compares the load-displacement hysteresis loops response for the tested T-beam with those obtained from the finite element analysis for the entire loading history for the same values of the shear transfer coefficients β_t and β_c .

It should be noted that the kinks in the load-deflection response and hysteresis curve shown in Figs. 6 and 7 at a load of about 10 kN represent the initiation of the flexural crack in the flange of the RC beam specimen (Tanarslan and Altin 2010).

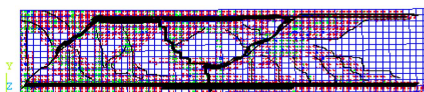
It is clear from Fig. 6 that the response envelope from the finite element analyses agreed very well with the experimental results. In general, the finite element model behaved stiffer and dissipated less energy (area enclosed by the hysteresis loops) than that of the experimental tested T-beam as indicated in Fig. 7. This small deviation in the displacement at failure between the FE and experimental results is very reasonable for such complex highly nonlinear analysis problem. The deviation between the experimental and finite element analysis results could be related to the concrete material model in ANSYS and the prescribed boundary conditions. The concrete material is defined in ANSYS as perfectly homogeneous for analytical work, but practically in real experimental work, they are heterogeneous. In addition, the prescribed boundary conditions might not simulate the accurate boundary conditions in the real experimental setup.

5.2 Prediction of crack evolution

The tested cantilever T-beam failed in shear with a typical shear crack occurring within the shear span. A thin first shear crack on the T-beam formed at 10 kN. At higher load increments, new shear and flexure cracks occurred on the T-beam. As the load reached 39.52 kN, three main shear cracks developed in shear span and T-beam failed consequently. The crack pattern of the tested and FE modeled T-beam at failure are shown in Figs. 8(a) and 8(b), respectively. Fig. 8(b) also shows a sketch of the cracks in the T-beam drawn on top of the cracks generated by the finite element model. The similarity of cracks pattern and accumulation between the experimentally tested



(a) Failure cracks pattern of tested T-beam



(b) Failure cracks pattern of finite element T-beam model

Fig. 8 Comparison of failure crack patterns of experimental and FE model of the T-beam

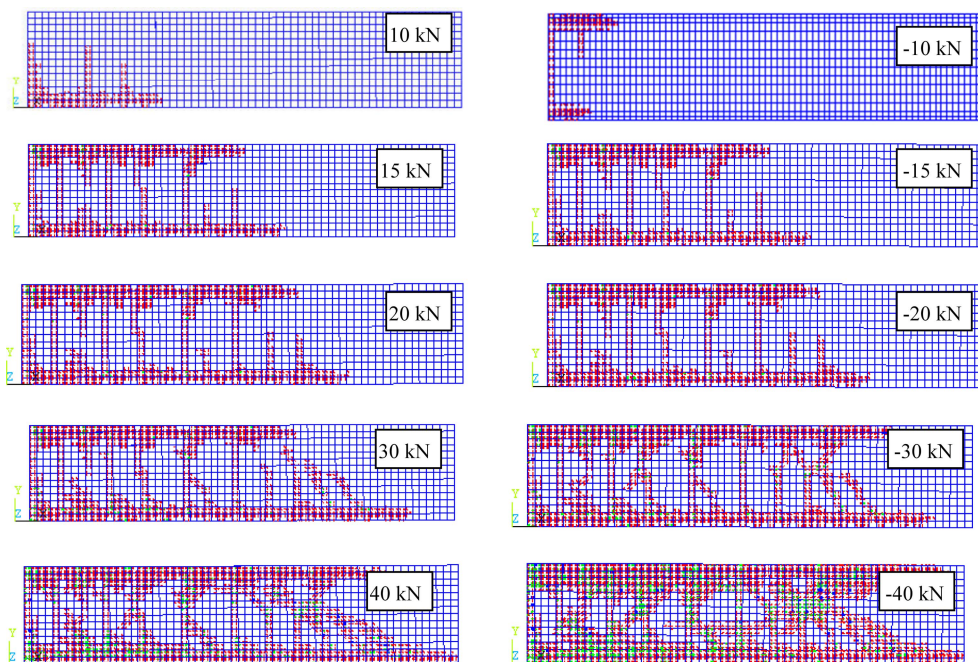


Fig. 9 Evolution of crack patterns of the T-beam

specimen and the finite element one is evident. The cracks orientations and their distribution along the T-beam is a clear indication of the cause of initiation of cracks and corresponding failure modes for the T-beam. The finite element ANSYS program is capable of recording the crack pattern of the beam at each applied load step including the peak load points during cyclic loading. Fig. 9 shows the evolutions of crack patterns developing in the tested T-beam during cyclic loading. The crack distribution predicted by the FE model at failure is also illustrated in Fig. 9.

It is clear from Figs. 8 and 9 that the crack orientation, distribution and patterns resulted from the

finite element analyses at the ultimate load step agrees very well with the experimental tested T-beam. The three major shear cracks developed in shear span of the tested T-beam are predicted by the FE model as shown in Figs. 8 and 9 which resulted in failure of the T-beam in shear. It is clear from Fig. 9 that numerous shear cracks occurred in the shear span of the T-beam during the cyclic loading which resulted in shear beam failure. In addition, other cracks occurred at the top and bottom (tension/compression) faces of the T-beam representing the crushing of the concrete cover during cyclic loading as shown in Figs. 8 and 9.

5.3 Parametric study

5.3.1 Variation of shear transfer coefficients

A parametric study was carried out on which β_t and β_c were varied over a certain range. As β_t increases the deflection decreases, especially for large load values as shown in Fig. 10(a).

Thus, the value of the open shear transfer coefficient β_t is a sensitive parameter in the concrete constitutive material model on the beam's vertical displacement. For small load values β_t has little effect if any on the free end displacement values. On the other hand, β_c does not have influence on the value of vertical displacement as shown in Fig. 10(b). The shear transfer coefficient β_t could be related to the change in the shear strain values in the concrete fibers along the plane of bending as presented in Fig. 10(c). It is clear from Fig. 10(c) that as β_t decreases the shear strain in the concrete decreases resulting in a shift of the neutral axis causing additional deflection. However, the

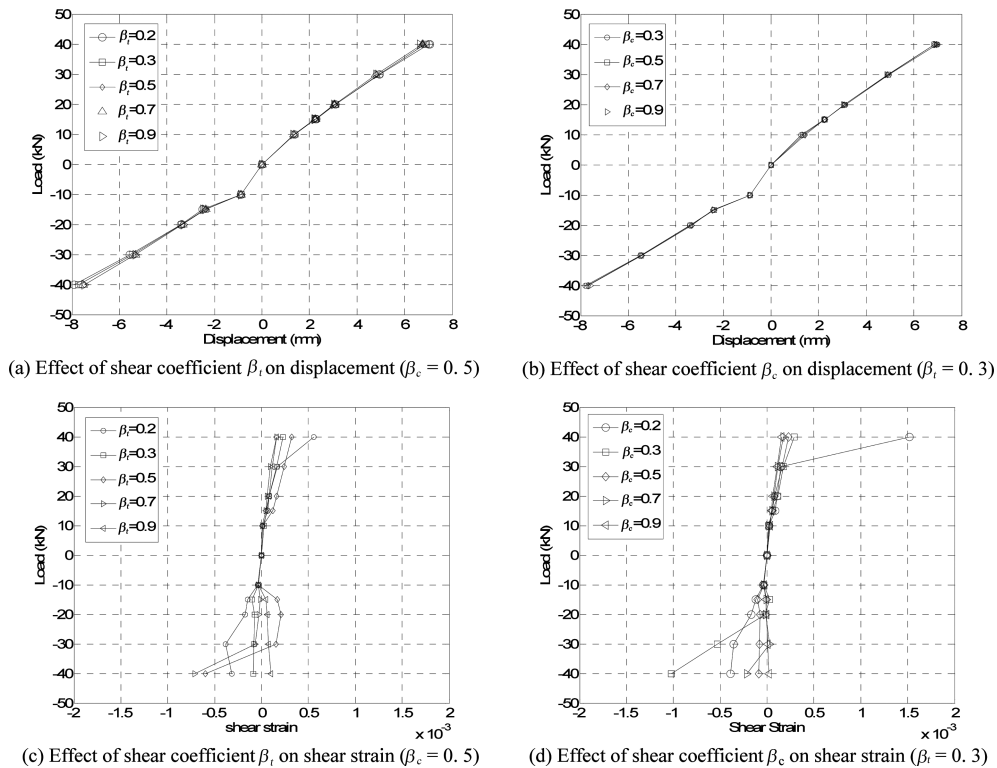


Fig. 10 Effect of shear coefficients β_t and β_c on the displacement and shear strain of the T-beam

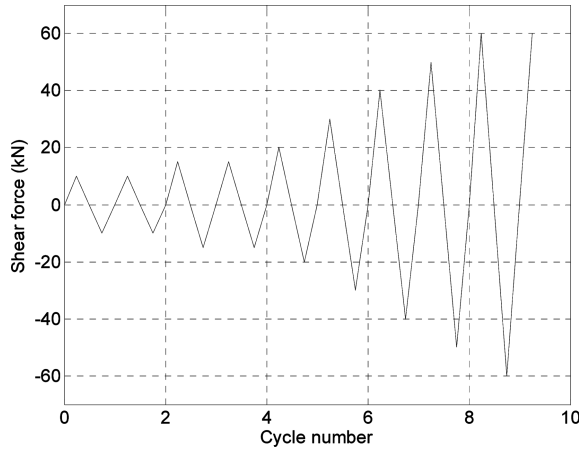


Fig. 11 Applied load cycles for the R-beam

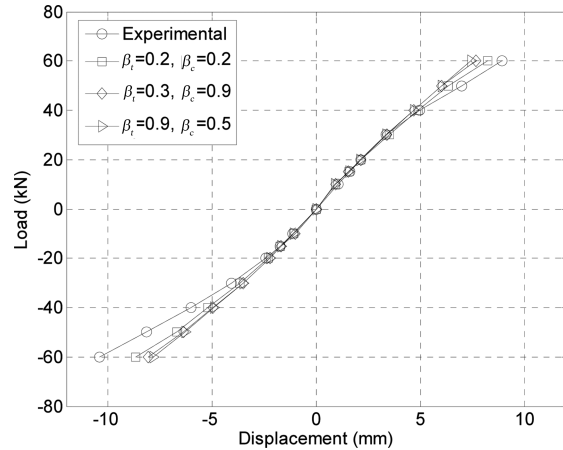


Fig. 12 Applied load versus measured and predicted displacement for the R-beam

shear transfer coefficient β_c has less profound effect in shear strain at all load values as shown in Fig. 10(d). In general, the effect of β_i and β_c on shear is more apparent than their effect in the maximum displacement. This mainly because the displacement is mainly flexure related rather than shear related.

5.3.2 Validation with rectangular cross section

In order to validate the choice of shear transfer coefficients of 0.2 as the optimum computational values to predict the experimental results, a rectangular cross section shear deficient beam (R-beam) is tested under cyclic loading shown in Fig. 11 which is different from the load history applied to the T-beam. The R-beam is 200 mm wide, 350 mm depth and 1700 mm long. The R-beam is reinforced with four 20 mm diameter bars in the compression zone and four 20 mm diameter bars in the tension zone. The R-beam had no internal shear reinforcing bars in the shear span. However, stirrups were provided outside the shear span to block local cracks that might occur due to applied load.

A finite element model was developed to predict the response of the R-beam and the analysis were performed for β_i and β_c of 0.2 and 0.2, 0.3 and 0.9, 0.9 and 0.5, respectively. The predicted results of the finite element analysis are compared with the experimental results as shown in Fig. 12.

It is clear from Fig. 12 that, when β_i and β_c are 0.2 and 0.2, the predicted result are closer to the experimental values, i.e., similar to the T-beam. Thus β_i and β_c are not geometry or load history dependent. Therefore, an optimum combination of the open and close crack shear transfer coefficients (β_i and β_c) of 0.2 are found to produce the best results compared to the experimental values.

5.3.3 Variation of concrete material compressive strength

In order to investigate the effect of concrete compressive strength on the performance of the T-beam, the model is solved for different values of concrete compressive strength (f'_c) of 25, 30.4, 35 and 45 MPa, respectively. The load deflection response envelop for all the studied case is shown in Fig. 13.

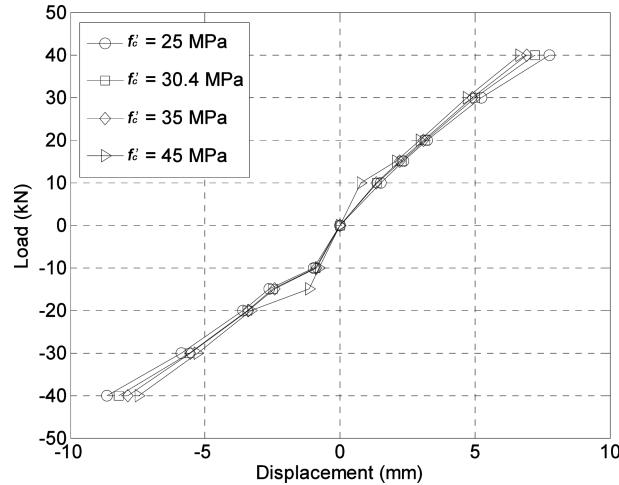


Fig. 13 Applied load versus measured and predicted displacement for the T-beam ($\beta_t = 0.2$, $\beta_c = 0.2$)

It is observed that as the concrete compressive strength increases the deflection decreases as expected. However, the percentage of decrease in deflection due to increase concrete compressive strength is not significant as shown in Fig. 13.

6. Conclusions

This paper presented a finite element prediction of response of reinforced concrete T-beam deficient in shear subjected to cyclic loading and compared it with experimental results. A parametric study was then conducted to investigate the sensitivity of both the open and close crack shear transfer coefficients (β_t and β_c) in the concrete material model and their effect on the shear strain and deflection of the T-beam. An optimum combination of the open and close crack shear transfer coefficients (β_t and β_c) needed for the constitutive material model for concrete to produce the best results comparable to the experimental results was found to be 0.2 for both. The results were also verified on a rectangular shear deficient beam (R-beam) tested under cyclic loading.

It can be concluded further from this investigation that:

- Cracks orientation, distribution and pattern of the finite element model are very close and resemble that of the experimental test.
- Response envelope of the finite element model and test data is also similar to each other. However, the finite element model has more stiffness than the experimental T-beam, resulting in less deflection values.
- The maximum free end deflection predicted by the finite element model is 1.7 mm (less than 1/16 inches) less than that of the tested experimental results. This is related to the assigned stiffness of the concrete material model. In general, this deviation from the experimental results is very reasonable for such complex and highly nonlinear behavior.
- In both the experiment and finite element analysis, the shear failure modes and mechanisms of the T-beam are similar to each other. The crack patterns at the final load from finite element model correspond well with the observed failure mode of the experimental T-beam.

- From these results it is obvious that the FE model with nonlinear constitutive models can be used to predict the load-displacement relation, the load capacity and failure mode of RC beams, accurately.
- The value of shear transfer coefficients, β_i and β_c , have variable effect on the free end displacement of the T-beam and on shear strain.
- When both shear transfer coefficients are equal to 0.2 the finite element result gave the best correlation to the experimental results for both beams irrespective of their geometry (T-beam, R-beam) or loading cycles.
- Variation of concrete compressive strength has little effect on the deflection.

In order to have extra validation of the developed FE model, further experimental tests are needed to be conducted in future research studies. The developed finite element models can be extended to investigate shear deficient beams strengthened with Carbon or Glass Fiber Reinforced Polymers (CFRP and GFRP) subjected to cyclic loading.

References

- Al-Ta'an, S.A. and Ezzadeen, N.A. (1995), "Flexural analysis of reinforced fibrous concrete members using the FE method", *Comput. Struct.*, **56**(6), 1065-1072.
- American Concrete Institute (ACI) (2005), *ACI 318-05 Building code requirements for structural concrete and commentary*, Farmington Hills, Michigan.
- ANSYS Version 11.0 (2007), *Finite element computer code*, ANSYS, Inc. Canonsburg, Pa. USA.
- ANSYS Workbench Version 11.0 (2007), *ANSYS workbench documentation*, ANSYS Inc. Canonsburg, Pa. USA ANSYS.
- ASCE Task Committee on Concrete and Masonry Structures (1982), *State of the art report on finite element analysis of reinforced concrete*, New York.
- Bangash, M.Y.H. (1989), "Concrete and concrete structures: numerical modeling and application", *Elsevier Science Publishers Ltd.*, London, UK.
- Bhatt, P. and Kader, M.A. (1998), "Prediction of shear strength of reinforced concrete beams by nonlinear Finite-element analysis", *Comput. Struct.*, **68**(1-3), 139-155.
- Cela, J. (1998), "Analysis of reinforced concrete structures subjected to dynamic loads with a viscoplastic Drucker-Prager model", *Appl. Math. Model.*, **22**(7), 495-515.
- Chen, D. (2006), "Computational framework for durability assessment of reinforced concrete structures under Coupled deterioration processes", PhD Thesis, Vanderbilt University, USA.
- Cotsovos, D.M., Zeris, C.A. and Abbas, A.A. (2009), "Finite element modelling of structural concrete", *Proceedings of COMPDYN 2009, ECCOMAS Thematic Conference on Computational Methods in Structural Dynamics and Earthquake Engineering Special Interest Conference M. Papadrakakis, M. Kojic, V. Papadopoulos (eds.)*, Rhodes, Greece, 22-24.
- Desayi, P. and Krishnan, S. (1964), "Equation for the stress-strain curve of concrete", *J. Am. Conc. Inst.*, **61**(3), 345-350.
- Fanning, P. (2001), "Nonlinear models of reinforced and post-tensioned concrete beams", *Electronic J. Struct. Eng.*, **2**, 111-119.
- Hawileh, R., Tanarlan, M., Naser, M. and Abdalla, J.A. (2011), "Experimental and numerical investigation on the performance of shear deficient RC beams strengthened with NSM GFRP reinforcement under cyclic loading", *3rd ECCOMAS Thematic Conference on Computational Methods in Structural Dynamics and Earthquake Engineering*, COMPDYN 2011, Corfu, Greece.
- Hawileh, R., Abdalla, J., Tanarlan, M. and Naser, M. (2010), "Modeling of nonlinear cyclic response of shear-deficient RC T-beams strengthened with side bonded CFRP fabric strips", *Comput. Concrete*, **8**(2), 193-206.
- Hawileh, R.A., A. Rahman, A. and Tabatabai, H. (2010), "Nonlinear finite element analysis and modeling of a

- precast hybrid beam-column connection subjected to cyclic loads”, *Appl. Math. Model.*, **34**(9), 2562-2583.
- Hawileh, R.A., Abdalla, J.A. and Tanarslan, M.H. (2009), “Finite element analysis of a shear deficient reinforced concrete beam subjected to dynamic loading”, *Proceedings of 2nd South-East European Conference on Computational Mechanics (SEECCM 2009)*, an IACM-ECCOMAS Special Interest Conference M. Papadrakakis, M. Kojic, V. Papadopoulos (eds.), Rhodes, Greece.
- Hu, H.T. and Schnobrich, W.C. (1990), “Nonlinear analysis of cracked reinforced concrete”, *ACI Struct. J.*, **87**(2), 99-207.
- Huang, Y., Kang, T.H.K., Ramseyer, C. and Rha, C. (2010), “Background to multi-scale modelling of unbonded post-tensioned concrete structures”, *Int. J. Theor. Appl. Muti. Mech.*, **1**(3), 219-230.
- Kachlakev, D.I. (2002), “Finite element analysis and model validation of shear deficient reinforced concrete beams strengthened with GFRP laminates”, *Proceedings of the Third International Conference on Composites in Infrastructure*, Paper 002, San Francisco, California, USA.
- Kim, W., Piyawat, K., Ramseyer, C. and Kang, T.H.K. (2010), “Experimental and numerical simulations of prestressed self-consolidating-concrete structures subject to nonlinear deformations”, *Int. J. Theor. Appl. Muti. Mech.*, **1**(4), 319-338.
- Kotsovos, M.D. and Pavlovic, M.N. (1986), “Non-linear finite element modeling of concrete structures: basic analysis, phenomenological insight, and design implications”, *Eng. Comput.*, **3**(3), 243-250.
- Kwak, H.G. and Filippou, F. (1990), *Finite element analysis of reinforced concrete structures under monotonis loads*, Report No. UCB/SEMM-90/14.
- Kwak, H.G. and Filippou, F. (1997), “Nonlinear FE analysis of R/C structures under monotonic loads”, *Comput. Struct.*, **65**(1), 1-16.
- Masti, K., Maghsoudi, A.A. and Rahgozar, R. (2008), “Nonlinear models and experimental investigation of lifetime history of HSC flexural beams”, *Am. J. Appl. Sci.*, **5**(3), 248-262.
- Naser, M., Hawileh, R., Abdalla, J.A. and Al-Tamimi, A. (2011), “Bond behavior of CFRP cured laminates: experimental and numerical investigation”, *J. Eng. Mater.-T ASME*, **134**(2), 021002.1-021002.9.
- Nilson, A.H. (1968), “Nonlinear analysis of reinforced concrete by the finite element method”, *J. Am. Concrete Inst.*, **65**(9), 757-766.
- Obidat, T.T., Heyden, S. and Dahlblom, O. (2010), “The effect of CFRP and CFRP/concrete interface models when modelling retrofitted RC beams with FEM”, *Compos. Struct.*, **65**(6), 1391-1398.
- Park, H. and Kim, J. (2005), “Hybrid plasticity model for reinforced concrete in cyclic shear”, *Eng. Struct.*, **27**(1), 35-48.
- Tanarslan, H.M. and Altin, S. (2010), “Behavior of RC T-section beams strengthened with CFRP strips subjected to cyclic load”, *Mater. Struct.*, **43**(4), 529-542.
- Willam, K.J. and Warnke, E.D. (1975), “Constitutive model for the triaxial behavior of concrete”, *Proceedings, International Association for Bridge and Structural Engineering*, **19**, ISMES, Bergamo, Italy, 174.
- Zeinkiewicz, O.Z., Taylor, R.L. and Zhu, J.Z. (2005), *The finite element method: its basis and fundamentals*, Butterworth-Heinemann, Oxford, 6th edition.